nature genetics

Common genetic variants at the 11q13.3 renal cancer susceptibility locus influence binding of HIF to an enhancer of cyclin D1 expression

Johannes Schödel[1], Chiara Bardella[2], Lina K Sciesielski[1], Jill M Brown[3], Chris W Pugh[1], Veronica Buckle[3], Ian P Tomlinson[2,4], Peter J Ratcliffe[1] & David R Mole[1]

Although genome-wide association studies (GWAS) have identified the existence of numerous population-based cancer susceptibility loci, mechanistic insights remain limited, particularly for intergenic polymorphisms. Here, we show that polymorphism at a remote intergenic region on chromosome 11q13.3, recently identified as a susceptibility locus for renal cell carcinoma[1], modulates the binding and function of hypoxia-inducible factor (HIF) at a previously unrecognized transcriptional enhancer of *CCND1* (encoding cyclin D1) that is specific for renal cancers characterized by inactivation of the von Hippel–Lindau tumor suppressor (pVHL). The protective haplotype impairs binding of HIF-2, resulting in an allelic imbalance in cyclin D1 expression, thus affecting a link between hypoxia pathways and cell cycle control.

Kidney cancer (renal cell carcinoma (RCC)) accounts for more than 100,000 deaths per year worldwide[2]. More than 80% are clear cell tumors (ccRCCs), and most are associated with loss of function of pVHL[3,4]. pVHL is a ubiquitin ligase that promotes oxygen-dependent degradation of HIF-1α and HIF-2α by recognizing hydroxylated prolyl residues in HIF-α (refs. 5–7). Loss of pVHL function upregulates HIF-α subunits and activates HIF-dependent transcriptional pathways. The frequency but uncertain or poorly understood causality of dysregulated hypoxia pathways in cancer has raised fundamental questions as to whether and by what means the HIF pathway contributes to ccRCC. A range of other (non-HIF) functions have been identified for pVHL[8] that may contribute to tumor suppressor behavior, but gene transfer and knockdown studies point to a role for HIF-2 but not HIF-1 in the progression of ccRCC xenografts[8–13]. However, to date, there has been little evidence from human genetic studies of a direct causal role for HIF in sporadic ccRCC. Genetic analyses of RCC tumor material have not identified activating mutations in *EPAS1* (encoding HIF-2α) and, unexpectedly, the only genetic alterations in genes encoding HIF subunits have been inactivating mutations or deletions of *HIF1A* (encoding HIF-1α)[13–16].

A recent GWAS discovered two SNPs in intron 1 of *EPAS1* that were significantly associated with increased RCC risk; however, no functional studies were performed[1]. In the same study, a second RCC susceptibility locus was identified in an intergenic region of unknown function at 11q13.3, a finding that has recently been replicated in other populations[17,18]. As part of an ongoing study to define the direct transcriptional targets of HIF-2 in renal cancer, we undertook a genome-wide analysis of HIF-2-binding sites in pVHL-defective 786-O cells (which lack functional HIF-1α owing to a truncated transcript[13]) using chromatin immunoprecipitation (ChIP) with antibodies to HIF-2α and its dimerization partner HIF-1β coupled to high-throughput sequencing (ChIP-seq).

Among ~600 pangenomic HIF-2 ChIP signals, we observed strong binding (ranked twelfth by peak height) almost precisely coinciding with the RCC predisposition SNP rs7105934 at 11q13.3. The strongest signal (H) was 5 kb centromeric to rs7105934 (chr. 11: 68943716–68944005). There were more minor signals immediately adjacent (h1) and more distal (h2) to this region (**Fig. 1a**). None of these regions bound HIF subunits in a previous ChIP-seq analysis in pVHL-competent MCF-7 breast cancer cells[19]. Analysis of data from Europeans in the 1000 Genomes project showed that the major ChIP-seq signal (H) overlapped polymorphic nucleotides rs7948643, rs7939721 and rs7939830, whereas the weaker signal (h2) overlapped rs17136556, rs77247065 and rs11263441. Pairwise linkage disequilibrium (LD) of all these SNPs and the RCC-associated SNP rs7105934 was reported to be high (r^2 = 1; from 1000 Genomes Pilot 1 data). To confirm this directly, we genotyped at each SNP a larger cohort of 192 cancer-free individuals from the UK and confirmed strong LD (r^2 ranging from 0.77 to 1), especially between rs7105934 and SNPs overlying the strongest HIF-2 ChIP signal (**Fig. 1a**). Sequence inspection indicated that sites H and h2 but not h1 contained consensus homeobox-responsive element (HRE) motifs (RCGTG; **Supplementary Fig. 1**). ChIP followed by quantitative PCR (ChIP-qPCR) confirmed robust binding of HIF-2α and HIF-1β

[1]Henry Wellcome Building for Molecular Physiology, University of Oxford, Oxford, UK. [2]Molecular and Population Genetics Laboratory, The Wellcome Trust Centre for Human Genetics, University of Oxford, Oxford, UK. [3]Weatherall Institute of Molecular Medicine, John Radcliffe Hospital and University of Oxford, Oxford, UK. [4]Oxford National Institute for Health Research (NIHR) Comprehensive Biomedical Research Centre, The Wellcome Trust Centre for Human Genetics, University of Oxford, Oxford, UK. Correspondence should be addressed to P.J.R. (pjr@well.ox.ac.uk), D.R.M. (drmole@well.ox.ac.uk) or J.S. (schoedel@well.ox.ac.uk).

Received 19 September 2011; accepted 30 January 2012; published online XX XXXX 2012; doi: 10.1038/ng.xxxx

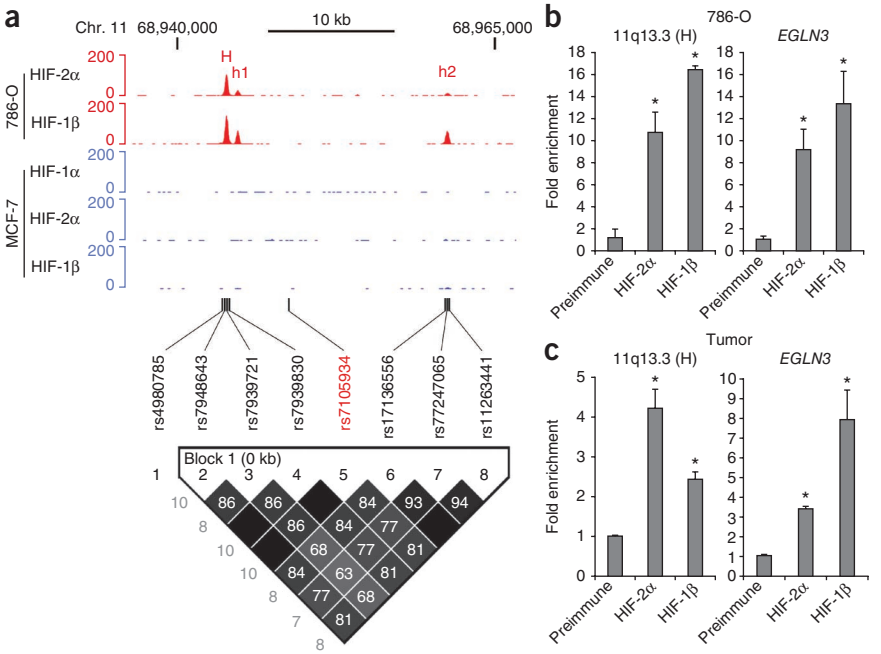

Figure 1 HIF binding at 11q13.3. (**a**) Genome Browser tracks showing the read density at the 11q13.3 locus for HIF-2α and HIF-1β ChIP-seq in 786-O cells (red). Also shown are read densities for HIF-1α, HIF-2α and HIF-1β ChIP-seq in MCF-7 cells in which HIF-α chains were stabilized by hydroxylase inhibition (blue). Three HIF-2α–binding sites (H, h1 and h2) are identified in 786-O cells but not MCF-7 cells. Also shown are the positions of genotyped SNPs, together with LD analysis (r^2 values). SNPs overlapping peaks H and h2 are in sufficiently strong LD with the disease-associated tag SNP rs7105934 (red) that the SNP can act as a simple proxy. (**b**,**c**) ChIP-qPCR analysis confirming HIF-2α and HIF-1β binding at 11q13.3 (H) in both 786-O cells (**b**) and renal tumor tissue (**c**). For comparison, ChIP-qPCR at an established HIF-binding site at the *EGLN3* locus[33,37] is shown. Bars show mean ± s.d. ($n = 3$); $^*P < 0.05$ compared to preimmune serum.

at the major site (H) in both 786-0 cells and human RCC tissue, whereas signals at h2 were much less robust, particularly for HIF-2α (**Fig. 1b**,**c** and data not shown). Thus, LD at the intergenic 11q13.3 RCC risk–associated locus extends across a region of robust HIF-2-binding (H) in RCC.

As this locus is remote from the nearest annotated gene and lacks CpG islands associated with gene promoters, we examined whether the major HRE-containing site (H) had the epigenetic characteristics of a transcriptional enhancer. First, we looked for reduced nucleosome occupancy using formaldehyde-assisted isolation of regulatory elements (FAIRE)[20]. This revealed a region of reduced nucleosome occupancy extending over approximately 2 kb around the HIF-binding site in 786-0 cells but not in MCF-7 cells, (**Fig. 2a**). Second, in

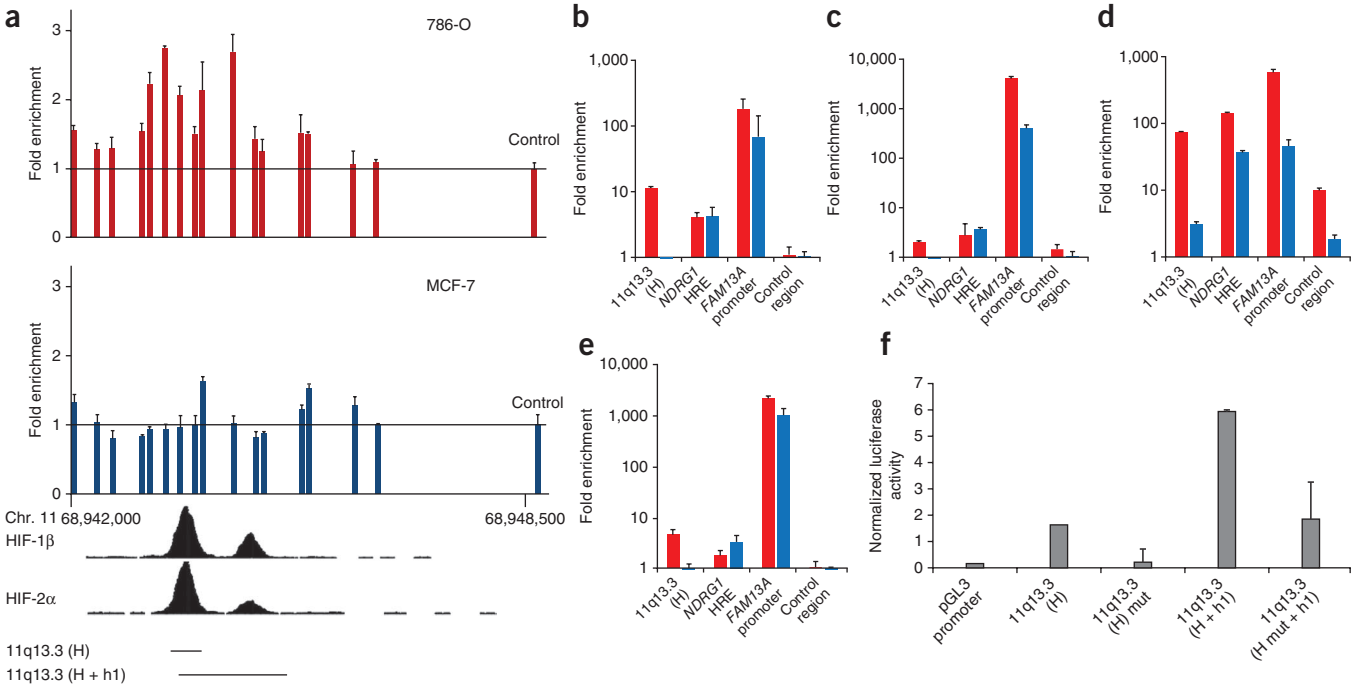

Figure 2 Chromatin structure and function of an enhancer at 11q13.3. (**a**) FAIRE was performed in 786-O cells (red) and MCF-7 cells (blue) to map nucleosome occupancy at the 11q13.3 locus. qPCR products were normalized to those obtained for input DNA at this locus and then related to values obtained at a nearby control region outside the putative enhancer (control). Data are plotted against chromosomal location; the positions of the ChIP-seq signals for HIF-1β and HIF-2α are shown below. (**b**–**e**) ChIP-qPCR signals at 11q13.3 (H) obtained from 786-O cells (red) or MCF-7 cells (blue) using antibodies to H3K4me1 (**b**), H3K4me3 (**c**), H3K27ac (**d**) and RNA Pol II (**e**). For comparison, signals at a ubiquitous HIF-binding enhancer (*NDRG1*; **Supplementary Fig. 3b**), a HIF-binding promoter (*FAM13A*) and a nearby non-enhancer control region are shown. Error bars, XX. (**f**) Luciferase reporter assay performed in 786-O cells using the sequences 11q13.3 (H) or 11q13.3 (H + h1). Mut, mutation of the core HRE motif in H. Data are normalized to activity from cotransfected β-galactosidase. Bars show mean ± s.d. ($n = 3$).

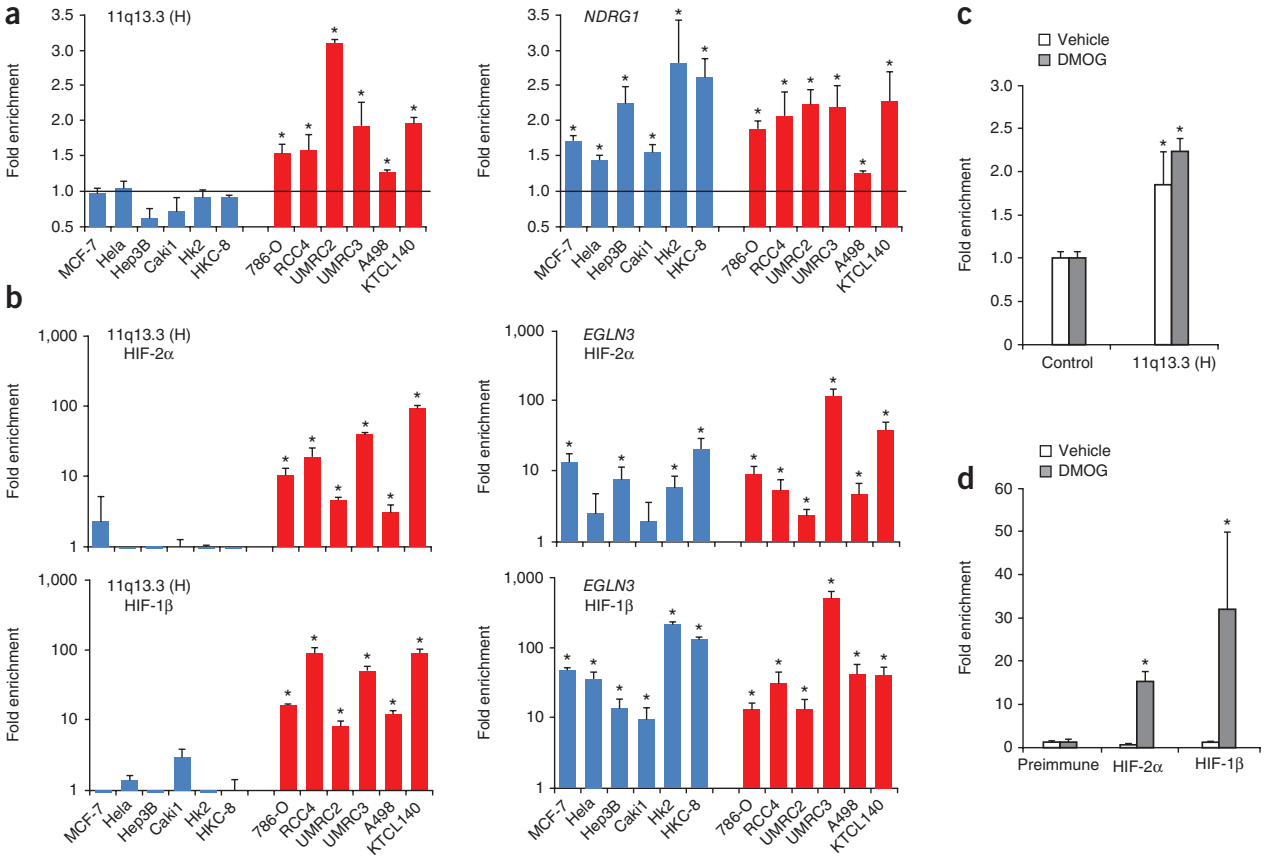

Figure 3 Cell type specificity of the 11q13.3 enhancer. (**a**) FAIRE analysis. Data are shown for a panel of six wild-type pVHL cell lines (blue) in which HIF was induced using HIF hydroxylase inhibitor, dimethyl oxalylglycine (DMOG), as well as six pVHL-defective cell lines (red). qPCR products were normalized as in **Figure 2a**. Enrichment value for primers centered on the ChIP-seq signal (H) are shown (left). For comparison, signals at the ubiquitous HIF-binding enhancer (*NDRG1*) are shown (right). (**b**) ChIP-qPCR results from the same panel of wild-type pVHL and pVHL-defective cell lines from **a** for HIF-2α (top) and HIF-1β (bottom) binding at 11q13.3 (H) (left). For comparison, signals at the *EGLN3* locus are shown (right). (**c**) FAIRE analysis in 786-O cells re-expressing wild-type pVHL (786-0/VHL cells). The enrichment value for primers centered on the ChIP-seq signal (H) normalized to the control (non-enhancer) site is shown. Cells were treated with or without DMOG to induce HIF. (**d**) ChIP-qPCR analysis for HIF-2α and HIF-1β at the 11q13.3 H peak in 786-0/VHL cells treated with or without DMOG. Bars are mean ± s.d. ($n = 3$); $^*P < 0.05$ relative to preimmune samples (ChIP) or to a control site (FAIRE).

786-0 cells but not MCF7 cells we observed high levels of monomethylated histone H3 at lysine 4 (H3K4me1) and acetylated H3 at lysine 27 (H3K27ac), with low levels of trimethylated histone H3 at lysine 4 (H3K4me3). This combination of histone modifications is observed at active enhancers (compare to the *NDRG1* enhancer) but not promoters (compare to the *FAM13A* promoter)[21–23] (**Fig. 2b–d**). As expected for an active enhancer, in 786-0 cells, there was a low-level ChIP-qPCR signal for RNA polymerase II (RNA Pol II), which is consistent with interaction with the transcriptional apparatus[21] (**Fig. 2e**). Finally, in 786-O cells, expression of a reporter gene was enhanced by these sequences and attenuated by mutation of the HRE (**Fig. 2f**). Taken together, these data indicate that the 11q13.3 RCC susceptibility locus overlaps a HIF-dependent transcriptional enhancer.

Genome-wide expression analysis in 786-O cells and renal tumors identified *CCND1* (encoding cyclin D1), which flanks the site of interest and lies 220 kb telomeric to the enhancer, as one of the most HIF-regulated genes on chromosome 11 (**Supplementary Fig. 2a,b**). *CCND1* is an oncogene that is commonly upregulated in cancer, including in RCC[24–26] (**Supplementary Fig. 2c**). Previous studies have defined *CCND1* as a HIF-regulated gene in 786-0 and other RCC cell lines but were unable to map the control sequences[10,27–30]. These analyses revealed notable cell type specificity; that is, *CCND1* is responsive to HIF-2α in RCC cells but not in any other cell analyzed.

We tested whether this tight cell type specificity was reflected in HIF-2 binding and the epigenetic enhancer marks at the 11q13.3 susceptibility locus. Both DNA accessibility, as determined by FAIRE, and HIF-2 binding, assessed by ChIP-qPCR, were similarly cell type specific, being present in all pVHL-defective RCC cell lines tested but absent across cell lines expressing wild-type pVHL (including cancerous (Caki-1) and noncancerous (HK-2 and HKC-8) renal epithelial cells) (**Fig. 3a,b**), despite comparable levels of HIF-2α induced by hydroxylase inhibition (**Supplementary Fig. 3a**). We observed similar cell type–specific patterns of HIF-1 binding: HIF-1 binding occurred in all pVHL-defective RCC cell lines that expressed this isoform but was absent in all cell lines expressing wild-type pVHL (**Supplementary Fig. 3c**). Furthermore, consistent with previously reported patterns of *CCND1* expression in RCC cell lines, the 11q13.3 enhancer remained accessible and able to bind HIF following reintroduction of wild-type pVHL into pVHL-defective RCC cells (786-0/VHL cells)[19,27] (**Fig. 3c,d**). Thus, constitutively high levels of HIF are not required to maintain the activity of this region as an enhancer, but it is a stable feature of cell lines derived from pVHL-defective RCC.

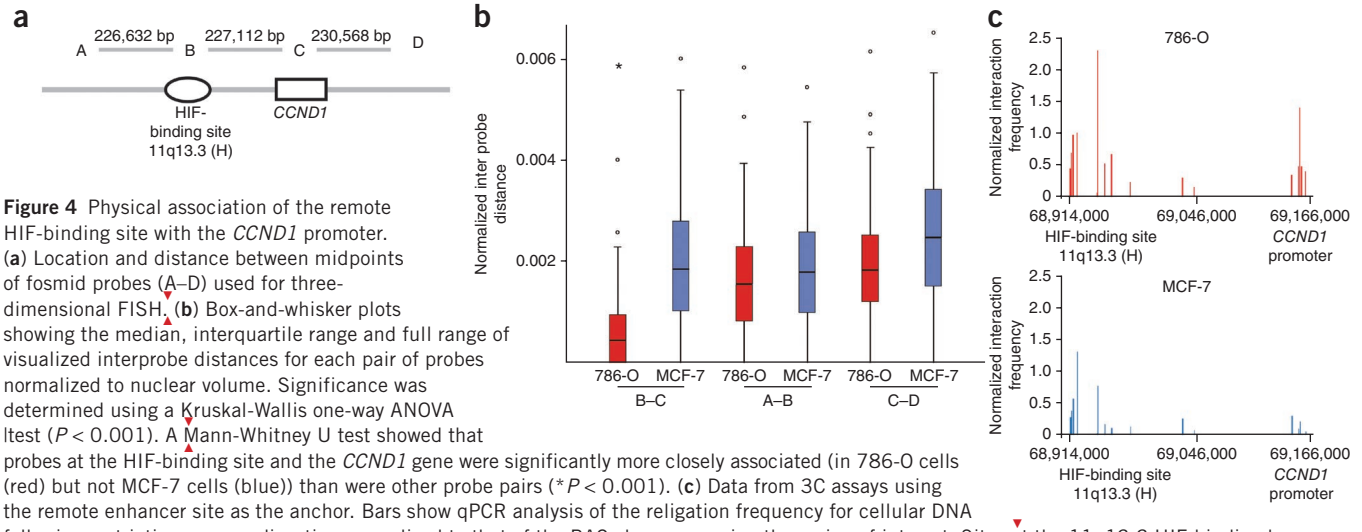

Figure 4 Physical association of the remote HIF-binding site with the *CCND1* promoter. (**a**) Location and distance between midpoints of fosmid probes (A–D) used for three-dimensional FISH. (**b**) Box-and-whisker plots showing the median, interquartile range and full range of visualized interprobe distances for each pair of probes normalized to nuclear volume. Significance was determined using a Kruskal-Wallis one-way ANOVA test ($P < 0.001$). A Mann-Whitney U test showed that probes at the HIF-binding site and the *CCND1* gene were significantly more closely associated (in 786-O cells (red) but not MCF-7 cells (blue)) than were other probe pairs (*$P < 0.001$). (**c**) Data from 3C assays using the remote enhancer site as the anchor. Bars show qPCR analysis of the religation frequency for cellular DNA following restriction enzyme digestion normalized to that of the BAC clones spanning the region of interest. Sites at the 11q13.3 HIF-binding locus preferentially ligated with fragments at the *CCND1* promoter in 786-O cells (red) but not in MCF-7 cells (blue), indicating a cell type–specific physical interaction.

Exact concordance between the existence of the HIF-binding enhancer and the regulation of cyclin D1 by HIF strongly suggested that the 11q13.3 locus encodes a long-range enhancer that physically associates with the *CCND1* promoter to regulate transcription. To test this, we used two assays of physical association between distant genetic loci: high-resolution FISH and chromatin conformation capture (3C)[31]. Both techniques provided evidence for physical association of the HIF-binding enhancer with the *CCND1* promoter in 786-O cells but not in MCF-7 cells (**Fig. 4** and **Supplementary Fig. 4**). Although our analysis does not exclude the possibility that the enhancer regulates additional genes, we conclude that the 11q13.3 susceptibility locus overlaps a cell type–specific long-range enhancer of cyclin D1 expression.

We next examined the effect of variants at 11q13.3 on the enhancer and on expression of *CCND1*. We first genotyped a number of pVHL-defective ccRCC cell lines at rs7105934, rs7948643 and rs77247065 and found one, KTCL140, to be heterozygous at all three SNPs (and at the remaining four SNPs covered by the other ChIP-seq peaks) with normal copy number and equal allelic dosage (**Supplementary Fig. 5**). Allele-specific analysis of immunoprecipitated chromatin in this cell line showed preferential binding of both HIF-2α and HIF-1β to the major (RCC-predisposing) allele at rs7948643 (**Fig. 5a**). ChIP using an antibody to RNA Pol II also showed that the major allele at this locus preferentially interacted with the basal transcriptional machinery (**Fig. 5b**). Furthermore, similar analysis of material prepared from KTCL140 cells by FAIRE indicated a greater

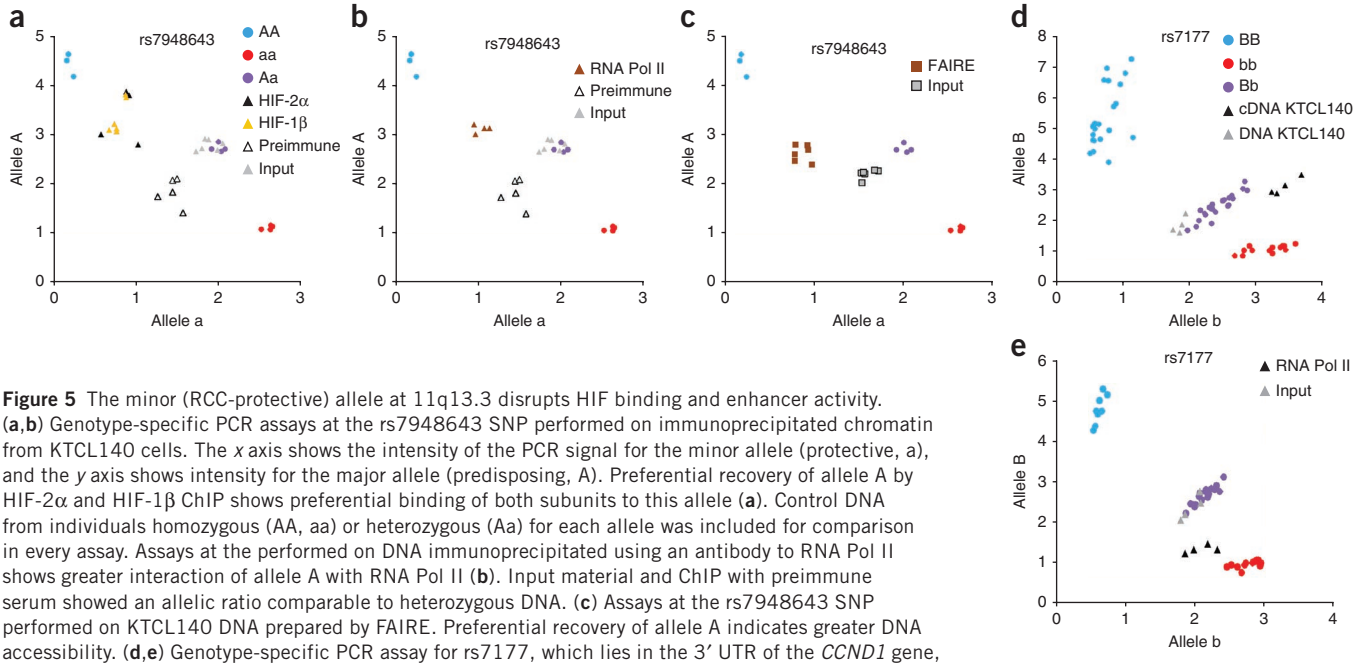

Figure 5 The minor (RCC-protective) allele at 11q13.3 disrupts HIF binding and enhancer activity. (**a**,**b**) Genotype-specific PCR assays at the rs7948643 SNP performed on immunoprecipitated chromatin from KTCL140 cells. The *x* axis shows the intensity of the PCR signal for the minor allele (protective, a), and the *y* axis shows intensity for the major allele (predisposing, A). Preferential recovery of allele A by HIF-2α and HIF-1β ChIP shows preferential binding of both subunits to this allele (**a**). Control DNA from individuals homozygous (AA, aa) or heterozygous (Aa) for each allele was included for comparison in every assay. Assays at the performed on DNA immunoprecipitated using an antibody to RNA Pol II shows greater interaction of allele A with RNA Pol II (**b**). Input material and ChIP with preimmune serum showed an allelic ratio comparable to heterozygous DNA. (**c**) Assays at the rs7948643 SNP performed on KTCL140 DNA prepared by FAIRE. Preferential recovery of allele A indicates greater DNA accessibility. (**d**,**e**) Genotype-specific PCR assay for rs7177, which lies in the 3′ UTR of the *CCND1* gene, using cDNA from KTCL140 cells (**d**) or DNA immunoprecipitated with an antibody to RNA Pol II (**e**) show allele-specific expression of *CCND1*. Genomic DNA from KTCL140 cells and control DNA from individuals homozygous (BB, bb) or heterozygous (Bb) for each allele were included for comparison. Each symbol represents an individual PCR assay.

degree of chromatin accessibility with the major allele at this locus (**Fig. 5c**). Thus, the minor (RCC-protective) allele at 11q13.3 disrupts HIF binding, DNA accessibility and interaction with the transcriptional apparatus at the *CCND1* enhancer.

We then determined whether these allele-specific effects at the *CCND1* enhancer alter the allelic balance of *CCND1* expression. We identified heterozygous SNPs (rs7177 and rs678653) within the 3′ UTR of *CCND1* in KTCL140 cells. These SNPs are in weak LD with SNPs at the HIF-binding site (for the tag SNP rs7105934, pairwise LD with rs7177, $r^2 = 0.02$, $D' = 0.51$ and with rs678653, $r^2 = 0.00$, $D' = 0.08$). The phase in KTCL140 cells is therefore unknown. However, mRNA from these cells showed distinct ($P < 1 \times 10^{-3}$) allelic imbalance compared to genomic DNA (**Fig. 5d** and **Supplementary Fig. 6a**). Furthermore, we observed similar allelic imbalance in binding of RNA Pol II to this coding region (**Fig. 5e** and **Supplementary Fig. 6b**). These results are therefore consistent with the prediction of differential *CCND1* expression arising from the two 11q13.3 alleles in these cells.

Taken together, these findings indicate that the activity of a promoter-distant enhancer of *CCND1* that binds HIF-2 in renal cancer is reduced by the protective haplotype at the 11q13.3 RCC-susceptibility locus. Given the established role of cyclin D1 as an oncogenic cell cycle regulator[26], this provides a plausible mechanism for the observed susceptibility effects. High LD in this region makes it difficult to distinguish the causative polymorphism(s) genetically. Although two of the SNPs in the susceptibility haplotype (rs7948643 and rs7939721) lie only 10 bp and 15 bp from the HIF-binding motif at 11q13.3 (H), respectively, neither disrupts the core RCGTG sequence. Thus, whether the minor allele affects HIF binding directly or indirectly by altering local chromatin structure remains to be determined. Notably, although, as with most HIF-binding sites, the enhancer can bind both HIF-1 and HIF-2, functional studies of *CCND1* expression suggest that only HIF-2 is transcriptionally active[10], a result which is in keeping with transcriptional selectivity among HIF isoforms being conferred by mechanisms triggered following DNA binding[32,33].

Although, we have not tested every cell with wild-type pVHL, the enhancer activity seems to be restricted to pVHL-defective RCC cells but is not reversed by reintroduction of pVHL, suggesting that it is a specific feature of the pVHL-defective RCC background. This raises questions as to when during RCC development the susceptibility effect operates and whether it contributes to the tissue specificity of pVHL tumor suppressor behavior. Kidneys of individuals with von Hippel–Lindau disease (the principal familial form of RCC) contain many tiny 'precursor lesions representing foci of biallelic *VHL* inactivation[34]. These manifest upregulation of the HIF pathway. However, only a minority express *EPAS1* and *CCND1*, and this pattern is strongly associated with dysplastic morphology[10]. This suggests several possibilities, at least in this form of RCC. First, the HIF-2–*CCND1* link may result from a 'second hit' occurring after biallelic *VHL* inactivation (perhaps owing to epigenetic alterations creating a 'neo-enhancer' (refs. 15,16,35,36)). Alternatively, the unusual connection between the HIF pathway and *CCND1* is an intrinsic property of a rare population of cells in the renal tubular epithelium that are then selected following dysregulation of the *VHL*-HIF pathway. A third possibility is that stable epigenetic changes are effected as a result of long-term HIF activation following pVHL inactivation and that these are not reversible upon re-expression of wild-type pVHL.

The finding that both major RCC-predisposition loci defined by GWAS at 2p21 (*EPAS1* encoding HIF-2α) and 11q13.3 affect specific components of hypoxia pathways suggests that particular aspects of hypoxia pathway dysregulation (as opposed to general upregulation) are important in RCC development. A third locus at 12q24.31 (within intron 1 of *SCARB1*) that was implicated in the original GWAS but not robustly in the replication cohorts[1] lies within 2 kb of an additional HIF-binding site identified in multiple cell types (**Supplementary Fig. 7**). However, LD with the candidate SNP at 12q24.31 did not extend over this HIF-binding region, indicating that, if this is an RCC predisposition locus, it is unlikely to operate through direct effects on HIF binding *per se*. Nevertheless, consideration of other GWAS signals in light of our pan-genomic analysis of HIF binding in RCC may yield further insights into the role of hypoxia pathways in RCC predisposition.

URLs. 1000 Genomes Project, http://www.1000genomes.org/; CisGenome, http://www.biostat.jhsph.edu/~hji/cisgenome/; Haploview, http://www.broadinstitute.org.

METHODS

Methods and any associated references are available in the online version of the paper at http://www.nature.com/naturegenetics/.

Accession codes. HIF ChIP-seq data have been deposited in the Gene Expression Omnibus, including data from 786-O cells (GSE34871) and MCF-7 cells (GSE28352).

Note: Supplementary information is available on the Nature Genetics website.

ACKNOWLEDGMENTS

Samples of renal tumors were a gift from A.L. Harris through the Oxford Radcliffe Biobank, Oxford Biomedical Research Centre. HKC-8 cells were provided by L. Racusen, 786-O cells re-expressing pVHL were a gift from W.G. Kaelin Jr., RCC4 cells were a gift from C.H. Buys, and all other RCC cells were from M. Lerman. This work was funded by the Wellcome Trust (088182/Z/09/Z, 078333/Z/05/Z and WT091857MA to J.S.), the Higher Education Funding Council for England, the German Research Foundation (SC 132/2-1 to L.K.S.) and by Urology Cancer Research and Education (UCARE).

AUTHOR CONTRIBUTION

J.S., C.W.P., V.B., I.P.T., P.J.R. and D.R.M. designed research. J.S., C.B., L.K.S., J.M.B., V.B. and D.R.M. performed experiments. J.S., C.B., L.K.S., J.M.B., V.B., I.P.T., P.J.R. and D.R.M. analyzed data. J.S., P.J.R. and D.R.M. wrote the manuscript.

COMPETING FINANCIAL INTERESTS

The authors declare no competing financial interests.

Published online at http://www.nature.com/naturegenetics/.
Reprints and permissions information is available online at http://www.nature.com/reprints/index.html.

1. Purdue, M.P. *et al.* Genome-wide association study of renal cell carcinoma identifies two susceptibility loci on 2p21 and 11q13.3. *Nat. Genet.* **43**, 60–65 (2011).
2. Ferlay, J. *et al.* Estimates of worldwide burden of cancer in 2008: GLOBOCAN 2008. *Int. J. Cancer* **127**, 2893–2917 (2010).
3. Gnarra, J.R. *et al.* Mutations of the *VHL* tumour suppressor gene in renal carcinoma. *Nat. Genet.* **7**, 85–90 (1994).
4. Herman, J.G. *et al.* Silencing of the *VHL* tumor-suppressor gene by DNA methylation in renal carcinoma. *Proc. Natl. Acad. Sci. USA* **91**, 9700–9704 (1994).
5. Maxwell, P.H. *et al.* The tumour suppressor protein VHL targets hypoxia-inducible factors for oxygen-dependent proteolysis. *Nature* **399**, 271–275 (1999).
6. Jaakkola, P. *et al.* Targeting of HIF-α to the von Hippel-Lindau ubiquitylation complex by O_2-regulated prolyl hydroxylation. *Science* **292**, 468–472 (2001).
7. Ivan, M. *et al.* HIFα targeted for VHL-mediated destruction by proline hydroxylation: implications for O_2 sensing. *Science* **292**, 464–468 (2001).
8. Kaelin, W.G. Jr. The von Hippel-Lindau tumour suppressor protein: O_2 sensing and cancer. *Nat. Rev. Cancer* **8**, 865–873 (2008).
9. Kondo, K., Kim, W.Y., Lechpammer, M. & Kaelin, W.G. Jr. Inhibition of HIF2α is sufficient to suppress pVHL-defective tumor growth. *PLoS Biol.* **1**, E83 (2003).
10. Raval, R.R. *et al.* Contrasting properties of hypoxia-inducible factor 1 (HIF-1) and HIF-2 in von Hippel-Lindau-associated renal cell carcinoma. *Mol. Cell. Biol.* **25**, 5675–5686 (2005).

11. Yan, Q., Bartz, S., Mao, M., Li, L. & Kaelin, W.G. Jr. The hypoxia-inducible factor 2α N-terminal and C-terminal transactivation domains cooperate to promote renal tumorigenesis *in vivo*. *Mol. Cell. Biol.* **27**, 2092–2102 (2007).
12. Gordan, J.D. *et al.* HIF-α effects on c-Myc distinguish two subtypes of sporadic *VHL*-deficient clear cell renal carcinoma. *Cancer Cell* **14**, 435–446 (2008).
13. Shen, C. *et al.* Genetic and functional studies implicate HIF1α as a 14q kidney cancer suppressor gene. *Cancer Discov.* **1**, 222–235 (2011).
14. Morris, M.R. *et al.* Mutation analysis of hypoxia-inducible factors *HIF1A* and *HIF2A* in renal cell carcinoma. *Anticancer Res.* **29**, 4337–4343 (2009).
15. Dalgliesh, G.L. *et al.* Systematic sequencing of renal carcinoma reveals inactivation of histone modifying genes. *Nature* **463**, 360–363 (2010).
16. Varela, I. *et al.* Exome sequencing identifies frequent mutation of the SWI/SNF complex gene *PBRM1* in renal carcinoma. *Nature* **469**, 539–542 (2011).
17. Wu, X. *et al.* A genome-wide association study identifies a novel susceptibility locus for renal cell carcinoma on 12p11.23. *Hum. Mol. Genet.* **21**, 456–462 (2012).
18. Cao, Q. *et al.* Chromosome 11q13.3 variant modifies renal cell cancer risk in a Chinese population. *Mutagenesis* published online (30 November 2011), doi:10.1093/mutage/ger085.
19. Schödel, J. *et al.* High-resolution genome-wide mapping of HIF-binding sites by ChIP-seq. *Blood* **117**, e207–e217 (2011).
20. Giresi, P.G., Kim, J., McDaniell, R.M., Iyer, V.R. & Lieb, J.D. FAIRE (formaldehyde-assisted isolation of regulatory elements) isolates active regulatory elements from human chromatin. *Genome Res.* **17**, 877–885 (2007).
21. Heintzman, N.D. *et al.* Distinct and predictive chromatin signatures of transcriptional promoters and enhancers in the human genome. *Nat. Genet.* **39**, 311–318 (2007).
22. Creyghton, M.P. *et al.* Histone H3K27ac separates active from poised enhancers and predicts developmental state. *Proc. Natl. Acad. Sci. USA* **107**, 21931–21936 (2010).
23. Rada-Iglesias, A. *et al.* A unique chromatin signature uncovers early developmental enhancers in humans. *Nature* **470**, 279–283 (2011).
24. Gumz, M.L. *et al.* Secreted frizzled-related protein 1 loss contributes to tumor phenotype of clear cell renal cell carcinoma. *Clin. Cancer Res.* **13**, 4740–4749 (2007).
25. Kaelin, W.G. Jr. Treatment of kidney cancer: insights provided by the VHL tumor-suppressor protein. *Cancer* **115**, 2262–2272 (2009).
26. Musgrove, E.A., Caldon, C.E., Barraclough, J., Stone, A. & Sutherland, R.L. Cyclin D as a therapeutic target in cancer. *Nat. Rev. Cancer* **11**, 558–572 (2011).
27. Zatyka, M. *et al.* Identification of cyclin D1 and other novel targets for the von Hippel-Lindau tumor suppressor gene by expression array analysis and investigation of cyclin D1 genotype as a modifier in von Hippel-Lindau disease. *Cancer Res.* **62**, 3803–3811 (2002).
28. Bindra, R.S., Vasselli, J.R., Stearman, R., Linehan, W.M. & Klausner, R.D. VHL-mediated hypoxia regulation of cyclin D1 in renal carcinoma cells. *Cancer Res.* **62**, 3014–3019 (2002).
29. Baba, M. *et al.* Loss of von Hippel-Lindau protein causes cell density dependent deregulation of CyclinD1 expression through hypoxia-inducible factor. *Oncogene* **22**, 2728–2738 (2003).
30. Wykoff, C.C. *et al.* Gene array of VHL mutation and hypoxia shows novel hypoxia-induced genes and that cyclin D1 is a VHL target gene. *Br. J. Cancer* **90**, 1235–1243 (2004).
31. Dekker, J., Rippe, K., Dekker, M. & Kleckner, N. Capturing chromosome conformation. *Science* **295**, 1306–1311 (2002).
32. Hu, C.J., Sataur, A., Wang, L., Chen, H. & Simon, M.C. The N-terminal transactivation domain confers target gene specificity of hypoxia-inducible factors HIF-1α and HIF-2α. *Mol. Biol. Cell* **18**, 4528–4542 (2007).
33. Lau, K.W., Tian, Y.M., Raval, R.R., Ratcliffe, P.J. & Pugh, C.W. Target gene selectivity of hypoxia-inducible factor-α in renal cancer cells is conveyed by post-DNA-binding mechanisms. *Br. J. Cancer* **96**, 1284–1292 (2007).
34. Mandriota, S.J. *et al.* HIF activation identifies early lesions in VHL kidneys: evidence for site-specific tumor suppressor function in the nephron. *Cancer Cell* **1**, 459–468 (2002).
35. Xia, X. *et al.* Integrative analysis of HIF binding and transactivation reveals its role in maintaining histone methylation homeostasis. *Proc. Natl. Acad. Sci. USA* **106**, 4260–4265 (2009).
36. Krieg, A.J. *et al.* Regulation of the histone demethylase JMJD1A by hypoxia-inducible factor 1 α enhances hypoxic gene expression and tumor growth. *Mol. Cell. Biol.* **30**, 344–353 (2010).
37. Pescador, N. *et al.* Identification of a functional hypoxia-responsive element that regulates the expression of the egl nine homologue 3 (*egln3*/*phd3*) gene. *Biochem. J.* **390**, 189–197 (2005).

ONLINE METHODS

Cell culture. We purchased 786-O cells and MCF-7 cells from the American Type Culture Collection (ATCC). HKC-8 cells were provided by L. Racusen, 786-O cells re-expressing pVHL were a gift from W.G. Kaelin Jr., RCC4 cells were a gift from C.H. Buys, and all other RCC cells were from M. Lerman. All cell lines were grown in DMEM supplemented with 100 U/ml penicillin, 100 µg/ml streptomycin and 10% FBS (Sigma). HKC-8 cells were cultured Q15 in DMEM and Ham's F-12 supplemented with 10% FCS, 2 mM L-glutamine, 100 U/ml penicillin and 100 µg/ml streptomycin, 5 µg/ml insulin, 5 µg/ml Q16 transferrin, and 5 ng/ml selenium (Sigma). Subconfluent cell cultures were exposed to 1 mM DMOG (Frontier Scientific) or 1% O_2 for 16 h before cell collection.

Tumor samples. Tumor samples were provided by A.L. Harris and collected in accordance with the World Medical Association Declaration of Helsinki.

Chromatin immunoprecipitation. ChIP was performed on cell lines as described[19,38], using antibodies to HIF-1α (PM14), HIF-2α (PM9) and HIF-1β (NB100-110) (all from Novus Biologicals), RNA polymerase II (Santa Cruz, sc-899), H3K4me1 (Abcam, ab8895), H3K4me3 (Cell signaling Technology, Q17 9751) and H3K27ac (Abcam, ab4729). Preimmune serum or IgG (Millipore, 12-370) were used as negative controls as applicable. For ChIP from tumors, snap-frozen tissue was pulverized, resuspended in PBS and fixed with 1% formaldehyde for 12 min at 4 °C. Cross-linking was quenched by addition of 125 mM glycine. After washing in PBS, the tissue was lysed in SDS buffer for 15 min at room temperature and sheared using an Ultra-Turrax. Sonication was carried out as described[19]. For each immunoprecipitation, we used the volume of chromatin corresponding to 25 mg of initial tissue weight.

High-throughput sequencing. Library preparations and sequencing was carried out as described[19]. Sequences were mapped to NCBI build 36 (hg18). We Q18 identified two-sample peaks using the CisGenome software suite.

RNA isolation and expression arrays. RNA was isolated using Tri Reagent (Sigma) and transcribed into cDNA using the high-capacity cDNA reverse transcription kit (Applied Biosystems). Microarray analysis of 786-O cells treated with control small interfering RNA (siRNA) or siRNA targeting HIF-2α, and of 786-O cells and VHL cells exposed to normoxia and hypoxia (1% O_2) for 16 h was carried out in triplicate using the Illumina WG6 Bead Chip at the microarray facility of the Wellcome Trust Centre for Human Genetics, and values were normalized and filtered for 'present' or 'absent' calls using Affymetrix software.

Immunoblotting. Cells were lysed in UREA and SDS buffer, and proteins were resolved by SDS-PAGE. After transferring the proteins onto polyvinylidene fluoride (PVDF) membranes, HIF proteins were detected using mouse monoclonal antibodies to HIF-1α (610958) and HIF-2α (190b) (both from BD Bioscience) and horseradish peroxidase–conjugated secondary antibodies (Dako).

Formaldehyde-assisted isolation of regulatory elements (FAIRE). We used an aliquot from cross-linked and sonicated ChIP chromatin, as described[20]. DNA was extracted with phenol-chloroform and then precipitated and puri- Q19 fied using a PCR product clean up kit (Sigma). We carried out qPCR on FAIRE DNA and input DNA in which cross-linking was reversed before phenol-chloroform extraction. Values were normalized to input DNA and compared to a region just outside the putative regulatory region (for 11q13.3, hg18 chr. 11: 68948541–68948669; for *NDRG1*, hg18 chr. 8: 134458206–134458299). Primer sequences are available on request.

Transfection assays. Transfections of plasmids and a β-galactosidase reporter Q20 were performed in 786-O cells using FuGENE 6 reagent (Roche). Cells were collected after 48 h, and the luciferase activity in extracts was measured using a luciferase reporter assay system (Promega). Values were normalized to β-galactosidase activity. Sequences were ligated into the Bgl2 restriction site Q21 of the pGL3 promoter vector (Promega) using PCR-amplified genomic DNA from 786-O cells spanning 227 bp (hg18 chr. 11: 68943675–68943901) of the major peak (H) or 1,453 bp (hg18 chr. 11: 68943675–68945127) including both the major (H) and minor (h1) peaks. Mutations of HREs (RCGTG into RCATA) were performed using site-directed mutagenesis. All constructs were sequence verified. Primer sequences are available on request.

DNA FISH. Fosmids spanning the region of interest were labeled by nick translation with biotin or digoxigenin as described[39] (*CCND1* gene: G248P85537B2, hg18 chr. 11: 69147108–69190642; HIF-binding site: G248P83053H10, hg18 chr. 11: 68921622–68961904; 227 kb centromeric of HIF-binding site: G248P85591A1, hg18 chr. 11: 68697196–68733066; and 227 kb telomeric of *CCND1* gene: G248P89319G2, hg18 chr. 11: 69380087–69418798). Two-dimensional FISH was performed as described[40], except that slides were denatured at 72 °C, and probes were denatured at 85 °C for 10 min. For each probe pair, interprobe distances were measured in micrometers using ImageJ software[41] in ~100 nuclei. Three-dimensional FISH was also performed as described[40], except that cells were permeabilized in 0.5% Triton X-100 in PBS followed by quenching in 0.276% ammonium chloride in PBS for 10 min at room temperature. Cells were denatured in a 1:4.5 dilution of concentrated HCl in milliQ water. Slides were hybridized overnight at 37 °C. Images were captured on a Zeiss 510 confocal microscope. *Z* stacks were taken of each nucleus at 400-nm steps. For each probe pair, interprobe distances were measured in micrometers using Zeiss LSM software, and nuclear volume measurements were performed in ImageJ software using the Voxel Counter plug-in in ~100 nuclei. Nonparametric statistical analysis was done using the Kruskal-Wallis one-way ANOVA test and the Mann-Whitney U test (IBM SPSS Statistics version 19). Q22

Chromatin conformation capture assay. Experiments were performed as described[42] with some modifications. Cells were grown in 15-cm dishes with (MCF-7) or without (786-O) 1 mM DMOG for 4 h. Cells were cross-linked using 1.5 mM Di(N-succinimidyl) glutarate (Sigma) for 45 min at room temperature followed by 1% formaldehyde (Sigma) for 10 min, and quenching was done using 0.125 M glycine (Sigma). After cell lysis, an EcoR1 (NEB) digest was carried out at 37 °C overnight. Fragments were diluted 1:8 in ligation buffer, and ligation was carried out for 4 h at 16 °C. Cross-linking was reversed at 65 °C overnight, and DNA was isolated using phenol-chloroform extraction. Digest efficiency was monitored using primers spanning the restriction sites and by comparison of digested to nondigested DNA. Chromatin interaction was interrogated by qPCR using a forward primer and a fluorescence-labeled probe located at the first EcoR1 restriction site downstream of the HIF-binding locus (anchor site) combined with reverse primers covering EcoR1 restriction sites across the region of interest. Two BAC clones (RP11 266K14 and RP11 378K8) covering the region of interest were used to create an artificial library of ligation products in order to normalize for PCR efficiency. Data were normalized to the signal from the BAC clone library and, between cell lines, by reference to a region at the *EEF1G* locus[43]. Primer sequences are available on request.

DNA extraction. DNA was extracted from blood samples using DNeasy Blood and Tissue (Qiagen), following the manufacturer's instructions. The DNA samples were quantified using PicoGreen (Invitrogen).

Allele-specific assays. LD of SNPs in the vicinity of the HIF-binding peaks (rs4980785, rs7948643, rs7939721, rs7939830, rs17136556, rs77247065 and rs11263441 with the tag SNP rs7105934 on 11q13.3 and rs4765621 with the tag SNP rs4765623 on 12q24.31) was verified in a cohort of 192 cancer-free control individuals using competitive allele-specific PCR KASPar chemistry (KBiosciences). Haploview software was used to define the haplotype blocks and recombination hotspots. To identify samples heterozygous for the common and rare alleles at rs7105934, rs7948643 and rs77247065, pVHL-defective ccRCC cell lines were genotyped using KASPar. For the heterozygous (1:1 allelic dosage) cell line KTCL140, genomic DNA derived from ChIP or FAIRE (two to three independent biological samples) or cDNA generated from DNase-treated mRNA was genotyped at rs7948643 and the *CCND1* 3′ UTR SNPs rs7177 and rs678653 using an allele-specific TaqMan assay (Applied Biosystems). Constitutional DNA from individuals known to be homozygous or heterozygous at each SNP was included in each assay as a reference. Information on all primers, probes and conditions used are available on request. We also analyzed

allele-specific expression at rs7177 as previously described[44], using one allele as test and the other as reference in a manner analogous to conventional qRT-PCR for mRNA expression levels based on a standard curve. This provided confirmatory evidence of the shift in allelic dosage found by TaqMan-based SNP analysis (data not shown). DNA from the KTCL140 cell line was also genotyped using the Illumina OmniExpress SNP array according to the manufacturer's protocols. Data were analyzed using the Illumina Genomestudio software.

Data analysis. Statistical analyses for FISH measurements were performed using IBM SPSS Statistics version 19. Statistical analyses for FAIRE and ChIP results were performed using a one-sample *t* test, comparing the mean with a hypothetical value of 1 using GraphPadPrism Version 4.00. All other analyses were conducted using a one-way Anova with Dunnett's post test.

38. Mole, D.R. *et al.* Genome-wide association of hypoxia-inducible factor (HIF)-1α and HIF-2α DNA binding with expression profiling of hypoxia-inducible transcripts. *J. Biol. Chem.* **284**, 16767–16775 (2009).
39. Brown, J. *et al.* Subtelomeric chromosome rearrangements are detected using an innovative 12-color FISH assay (M-TEL). *Nat. Med.* **7**, 497–501 (2001).
40. Brown, J.M. *et al.* Coregulated human globin genes are frequently in spatial proximity when active. *J. Cell Biol.* **172**, 177–187 (2006).
41. Abramoff, M.D., Magalhaes, P.J. & Ram, S.J. Image processing with ImageJ. *Biophotonics International* **11**, 36–42 (2004).
42. Hagège, H. *et al.* Quantitative analysis of chromosome conformation capture assays (3C-qPCR). *Nat. Protoc.* **2**, 1722–1733 (2007).
43. Ramachandrareddy, H. *et al. BCL6* promoter interacts with far upstream sequences with greatly enhanced activating histone modifications in germinal center B cells. *Proc. Natl. Acad. Sci. USA* **107**, 11930–11935 (2010).
44. Lo, H.S. *et al.* Allelic variation in gene expression is common in the human genome. *Genome Res.* **13**, 1855–1862 (2003).

Q34

doi:10.1038/ng.2204

QUERY FORM

Nature Genetics	
Manuscript ID	[Art. Id: 2204]
Author	
Editor	
Publisher	

AUTHOR:

The following queries have arisen during the editing of your manuscript. Please answer queries by making the requisite corrections directly on the galley proof. It is also imperative that you include a typewritten list of all corrections and comments, as handwritten corrections sometimes cannot be read or are easily missed. Please verify receipt of proofs via e-mail

Query No.	*Nature of Query*
Q1	Please carefully check the spelling and numbering of all author names and affiliations.
Q2	Sentence correct as edited?
Q3	Sentence correct as edited?
Q4	Correct as edited?
Q5	Correct as edited?
Q6	Parentheses have been removed here and below as they didn't seem to be necessary. OK?
Q7	Definition of HRE correct? Also, please define R in the motif sequence.
Q8	Please give a brief description of the reporter construct.
Q9	Correct as edited?
Q10	Sentence correct as edited?
Q11	RCC ok instead of renal cancer.
Q12	Correct as edited?
Q13	Splitting of overlong sentence. Ok?
Q14	Please provide a more specific link to the Haploview website.
Q15	Correct as edited?

QUERY FORM

Nature Genetics	
Manuscript ID	[Art. Id: 2204]
Author	
Editor	
Publisher	

AUTHOR:

The following queries have arisen during the editing of your manuscript. Please answer queries by making the requisite corrections directly on the galley proof. It is also imperative that you include a typewritten list of all corrections and comments, as handwritten corrections sometimes cannot be read or are easily missed. Please verify receipt of proofs via e-mail

Query No.	*Nature of Query*
Q16	Transferrin correct? Did read "transferring".
Q17	Correct that the first three antibodies in the list are all from Novus Biologicals?
Q18	Sentence correct as edited?
Q19	Please give the exact name of the kit.
Q20	Correct that FuGENE reagent is from Roche?
Q21	Which pGL3 vector, basic?
Q22	Correct as edited?
Q23	Please check that all funders have been appropriately acknowledged and that all grant numbers are correct.
Q24	Please provide affiliation information for all researchers providing materials.
Q25	Correct as edited?
Q26	Sentence correct as edited?
Q27	Please define error bars in b–e.
Q28	$n = 3$ transfections?
Q29	As meant?
Q30	Correct that A–D are the FISH probe names?

QUERY FORM

Nature Genetics	
Manuscript ID	[Art. Id: 2204]
Author	
Editor	
Publisher	

AUTHOR:

The following queries have arisen during the editing of your manuscript. Please answer queries by making the requisite corrections directly on the galley proof. It is also imperative that you include a typewritten list of all corrections and comments, as handwritten corrections sometimes cannot be read or are easily missed. Please verify receipt of proofs via e-mail

Query No.	*Nature of Query*
Q31	Sentence correct as edited?
Q32	Edit ok?
Q33	Please note combination of description of panels a and b to eliminate redundancy. Please adjust as needed.
Q34	This reference was not found in PubMed. Please check all details are correct. Alternatively, cite the URL http://rsbweb.nih.gov/ij/ in methods and renumber references.